Title

Photodynamic Therapy of Human Glioma Spheroids Using 5-Aminolevulinic Acid

Journal

Photochemistry and Photobiology, 72(1)

ISSN

0031-8655

Authors

Madsen, Steen J

Sun, Chung-Ho

Tromberg, Bruce J

et al.

Publication Date

2000

DOI

10.1562/0031-8655(2000)072<0128:ptohgs>2.0.co;2

Photochemistry and Photobiology, 2000, 72(1): 128–134

Photodynamic Therapy of Human Glioma Spheroids Using 5-Aminolevulinic Acid¶

Steen J. Madsen*[1,2], Chung-Ho Sun[3], Bruce J. Tromberg[3], Vincent P. Wallace[3] and Henry Hirschberg[3,4]

[1]Department of Health Physics, University of Nevada, Las Vegas, NV;
[2]University of Nevada, Las Vegas Cancer Institute, Las Vegas, NV;
[3]Beckman Laser Institute and Medical Clinic, University of California, Irvine, CA and
[4]Department of Neurosurgery, Rikshospitalet, Oslo, Norway

Received 5 January 2000; accepted 24 April 2000

ABSTRACT

The response of human glioma spheroids to 5-aminolevulinic acid (ALA)–mediated photodynamic therapy (PDT) is investigated. A two-photon fluorescence microscopy technique is used to show that human glioma cells readily convert ALA to protoporphyrin IX throughout the entire spheroid volume. The central finding of this study is that the response of human glioma spheroids to ALA-mediated PDT depends not only on the total fluence, but also on the rate at which the fluence is delivered. At low fluences ($\leq$50 J cm^{-2}), lower fluence rates are more effective. At a fluence of 50 J cm^{-2}, near-total spheroid kill is observed at fluence rates of as low as 10 mW cm^{-2}. The fluence rate effect is not as pronounced at higher fluences ($>$50 J cm^{-2}), where a favorable response is observed throughout the range of fluence rates investigated. The clinical implications of these findings are discussed.

INTRODUCTION

Primary intracranial neoplasms account for 2% of all cancer deaths (1). Approximately half of these are glioblastoma multiforme—the most aggressive variety of glial tumors (2). There is no satisfactory treatment for these infiltrative neoplasms. The best available treatment using surgery, chemotherapy and radiation therapy results in a median survival of 10 months (3). Five year survival rates are dismal ($<$5%). Failure of treatment is usually due to local recurrence at the site of surgical resection indicating that a more aggressive local therapy could be of benefit. In 80% of all cases, recurrence is within 2 cm of the resected margin (4). Several studies have shown that photodynamic therapy (PDT)† may prove to be useful in prolonging survival and/or improving the quality-of-life in glioma patients (5–11).

PDT has several features that may make it an effective adjuvant therapy in the treatment of brain tumors: (1) PDT is a localized form of treatment; the treatment volume is limited by high attenuation of light in brain tissues; (2) resistance to PDT has not been encountered during treatments of brain tumors (12); and (3) repeated applications of PDT is an option due to low long-term morbidity (12).

Porphyrins, such as hematoporphyrin derivative and Photofrin®, have been used almost exclusively in clinical PDT trials of the brain. Although favorable results have been reported by a number of clinicians (13,14) these photosensitizers have several drawbacks that may limit their applicability in certain situations. For example, the uncommonly long period of cutaneous photosensitization (lasting up to several weeks) observed in patients following administration of these photosensitizers, may preclude their use in fractionated PDT treatment regimens. Furthermore, the relatively poor tumor-to-normal tissue localization observed by several groups (15–17) may limit the effectiveness of these photosensitizers due to the potential of normal tissue complications. Due to the drawbacks of traditional porphyrins, other photosensitizers, such as boronated protoporphyrin and 5-aminolevulinic acid (ALA) are currently being evaluated for use in PDT of gliomas.

In ALA-induced endogenous photosensitization, the heme biosynthetic pathway is used to produce protoporphyrin IX (Pp IX)—a potent photosensitizer (18–20). Heme is synthesized from glycine and succinyl CoA. The rate-limiting step in the pathway is the conversion of glycine and succinyl CoA to ALA, which is under negative feedback control by heme (21). Through the introduction of ALA, the regulatory feedback system becomes overloaded causing an accumulation of Pp IX, which, when activated, causes the photosensitizing effect for PDT and porphyrin fluorescence for diagnosis.

ALA has been used primarily as a topical agent in the treatment of superficial skin lesions (22); however, the abundance of ALA-induced Pp IX in rapidly proliferating cells of many tissues provides a biologic rationale for ALA-mediated PDT in the treatment of a wide variety of lesions (21). The combination of excellent tumor-to-normal brain tissue

¶Posted on the web on 5 May 2000.
*To whom correspondence should be addressed at: Department of Health Physics, University of Nevada, Las Vegas, 4505 Maryland Pkwy., Box 453037, Las Vegas, NV 89154-3037, USA. Fax: 702-895-4819; e-mail: steenm@ccmail.nevada.edu
†*Abbreviations:* ALA, 5-aminolevulinic acid; BBB, blood-brain barrier; MBR, mitochondrial benzodiazepine receptor; PDT, photodynamic therapy; Pp IX, protoporphyrin IX.

localization (16), short period of skin phototosensitization (24–48 h) and the possibility of oral administration, makes ALA an ideal photosensitizer for use in fractionated PDT treatments of glioma patients.

The aim of PDT is to eliminate the nests of tumor cells remaining in the margins of the resection cavity. However, due to the high attenuation of light in the brain tissue (23), long treatment times are required in order to deliver sufficient light doses (fluences) to depths of 1–2 cm in the resection cavity. Furthermore, a number of *in vitro* (24,25) and *in vivo* (26–29) studies suggest that response to PDT depends not only on total fluence, but also on the rate at which the fluence is delivered—lower fluence rates appear more efficacious in many instances. Although fluence rate effects have been observed in numerous systems, a systematic study of such effects in a human glioma spheroid model using ALA has not been attempted.

In this study, the response of human glioma spheroids to ALA-mediated PDT is investigated. Of particular interest is the response of spheroids to the low fluence rates observed in the resected tumor margin during typical PDT treatments. To this end, spheroid survival and growth were monitored as functions of fluence and fluence rate. Two-photon fluorescence microscopy was used to (1) confirm the presence of Pp IX in individual glioma cells following incubation in ALA; and (2) evaluate Pp IX distributions in individual spheroids.

Spheroids were used in this study since they have a complexity intermediate to standard monolayer cultures and tumors *in vivo*. The three-dimensional arrangement of multicellular spheroids results in heterogeneous subpopulations of cells differing in their proliferation, nutrition and oxygenation status (30). Spheroids thus capture some of the characteristics of human tumors *in vivo*. However, since this is accomplished *in vitro*, the spheroid model allows various tumor cell–specific phenomena to be studied in the absence of complex host-dependent factors (31).

MATERIALS AND METHODS

Photosensitizer. In the PDT studies, spheroids were incubated in 1000 μg mL^{-1} of ALA (Sigma, St. Louis, MO) for approximately 4 h. ALA concentrations of 100 μg mL^{-1} were used in the two-photon fluorescence investigations.

Cell cultures. The grade IV GBM cell line (ACBT) used in this study was a generous gift of G. Granger (University of California, Irvine, CA). The cells were cultured in Dulbecco modified Eagle medium (Gibco, Grand Island, NY) with high glucose, and supplemented with 2 m*M* L-glutamine, penicillin (100 U mL^{-1}), streptomycin (100 μg mL^{-1}) and 10% heat-inactivated fetal bovine serum (Gibco). Cells were maintained at 37°C in a 7.5% CO_2 incubator. At a density of 70% confluence, cells were removed from the incubator and left at room temperature for approximately 20 min. The resultant cell clusters (consisting of approximately 10 cells) were transferred to a Petri dish and grown to tumor spheroids of varying sizes. Spheroids were grown according to standard techniques (32). Spheroids of two diameters (250 and 500 μm) were selected by passage through screen meshes (Sigma) of various sizes. It took approximately 14 and 21 days for spheroids to reach sizes of 250 and 500 μm, respectively. The spheroid culture medium was changed three times weekly.

PDT treatments. In all cases, spheroids were irradiated with 635 nm light from an argon ion–pumped dye laser (Coherent, Inc., Santa Clara, CA). Light was coupled into a 200 μm dia. optical fiber containing a microlens at the output end. Spheroids were exposed to fluences of 25, 50, 100 or 200 J cm^{-2} delivered at fluence rates of 10, 25, 50, 75, 150 or 200 mW cm^{-2}. Spheroids were irradiated in a Petri dish. A 2 cm dia. gasket was placed in the dish to confine the spheroids to the central portion of the dish and thus limit the extent of the irradiated field. Following irradiation, individual spheroids were placed into separate wells of a 96-well culture plate and monitored for growth. A microscope with a calibrated eyepiece micrometer was used to measure the spheroid diameter. Determination of the spheroid size was carried out by measuring two perpendicular diameters of each spheroid using a microscope with a calibrated eyepiece micrometer. Typically, 10–12 spheroids were followed for each irradiation condition. Since each trial was performed 3 or 4 times, a total of 30–50 spheroids were followed for a given set of parameters. Spheroids were followed for up to 35 days.

ALA distribution. The two-photon scanning fluorescence microscope system used to evaluate ALA distributions in individual spheroids has been described extensively elsewhere (33). Briefly, 100 fs light pulses of wavelength 800 nm are produced by a mode-locked titanium sapphire laser (Coherent, Inc.). The pulse train exiting the laser is expanded and collimated using two lenses to overfill the back aperture of the microscope objective. The beam is scanned across the sample, which is placed on an inverted Zeiss Axiovert 100 microscope (Zeiss, Thornwood, NY), using a personal computer–controlled X–Y scanner (Series 603X, Cambridge Technology, Inc., Watertown, MA). A 63×, 1.2 n.a. water immersion objective (C-Apochromat, Zeiss) having a working distance of 250 μm was used in this study. The two-photon fluorescence from the tissue was detected using a single-photon counting detection system consisting of two photomultiplier tubes (Hamamatsu Corp., Bridgewater, NJ) arranged perpendicularly. The tubes differ in their spectral sensitivity; one is optimized for green light (R7400P), the other for red light (R7400P-01). It is thus possible to detect fluorescence in two different wavelength regions simultaneously.

Pp IX fluorescence images were collected using the red channel and a 635 nm bandpass (20 nm full width at half maximum) filter (Chroma Technology Corp., Brattleboro, VT). Images were acquired at spheroid depths ranging from 40 to 120 μm. Depth discrimination was accomplished by adjusting the Z position of the water immersion objective. Image acquisition times were of the order of 20 s (20 frames at 1.0 s/frame). Normalized fluorescence signals were determined from the following formula:

$$N = \frac{I_s - I_b}{I_b}, \tag{1}$$

where I_s is the peak fluorescence signal observed from an ALA-incubated spheroid at a particular depth and I_b is the peak background fluorescence from a control spheroid at an equivalent depth.

Autofluorescence images were acquired using the green channel and a shortpass filter (SBG-39, CVI, Albuquerque, NM).

RESULTS

The strong red fluorescence signals (λ = 635 nm) observed following two-photon excitation of human glioma cells incubated in ALA indicate that these cells are capable of converting ALA to Pp IX (Fig. 1a). There appear to be several regions of intense fluorescence (denoted by red) adjacent to the large central nucleus (dark region). The autofluorescence image (Fig. 1b), acquired with a shortpass filter, is shown for comparative purposes. The bright areas are most likely due to reduced nicotinamide adenine dinucleotide fluorescence. Fluorescence was observed to spheroid depths of approximately 120 μm suggesting the presence of Pp IX throughout the entire spheroid volume (*ca* 250 μm dia.). As illustrated in Fig. 2, the fluorescence signal decreases with increasing depth. The rapid decline in signal with depth should not be interpreted as being due to decreasing drug levels; rather, it is attributed to attenuation due to scattering and absorption of light by the cells.

The growth rates of various control groups are illustrated

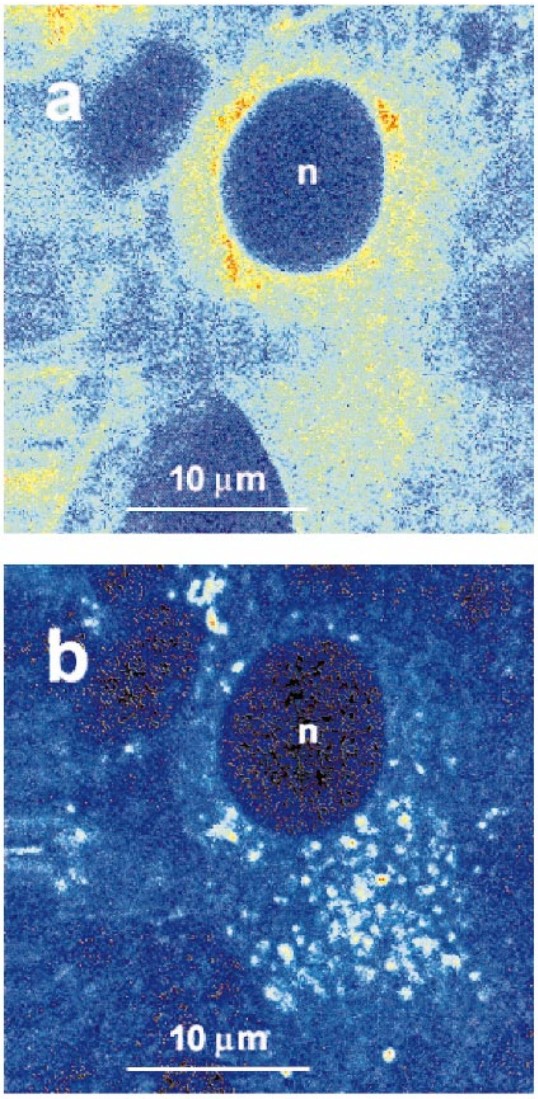

Figure 1. Two-photon fluorescence images (X–Y plane, Z = 40 μm) of human glioma spheroids showing (a) subcellular localization of Pp IX following incubation in 100 μg mL^{-1} ALA for 4 h and (b) detailed cellular structure from autofluorescence. The scan region is approximately 35 × 35 μm. The nucleus is denoted by ''n''.

in Fig. 3a,b. It is shown that neither light-only treatment nor drug-only treatment has any effect on spheroid growth. In both cases, growth rates are identical to those of the true controls, *i.e.* the untreated spheroids. As shown in Fig. 3a,b, glioma spheroids reach a limiting size of approximately 1500 μm, 25–30 days after treatment.

Effects of light fluence and fluence rate on spheroid survival are illustrated in Fig. 4. A spheroid is assumed to have survived treatment if it grows at any time during the observation period. Spheroids treated with light only, or drug only (dark controls) had identical survival to the true controls (no light, no drug). In all cases, 100% survival was observed (data not shown). As shown in Fig. 4a, spheroid survival is very sensitive to both fluence and fluence rate. At high fluences (Fig. 4b), the fluence rate dependence is minimal—significant spheroid kill is observed at all fluence rates. This is especially the case at the highest fluence investigated (200

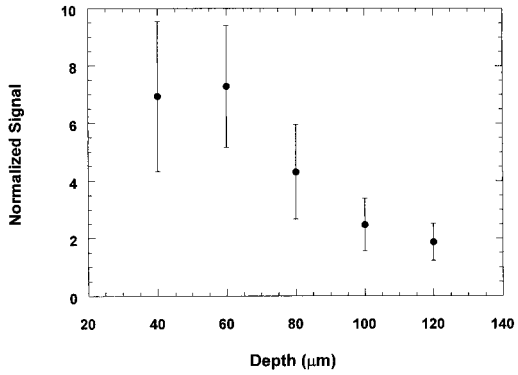

Figure 2. Normalized Pp IX fluorescence signal as a function of spheroid depth. Normalized signals were evaluated from the means of peak fluorescence signals acquired from five different ALA-incubated spheroids, and from peak background signals obtained from control spheroids. Standard deviations are indicated by the error bars.

J cm^{-2}). As the total fluence is decreased, however, the effects of fluence rate become more pronounced. At fluences of 50 J cm^{-2} and lower (Fig. 4a), it appears that lower fluence rates are more effective than higher ones. In other words, the threshold light dose can be decreased simply by giving the dose over a longer period of time, *i.e.* by lowering the fluence rate. It is interesting to note that, even at the

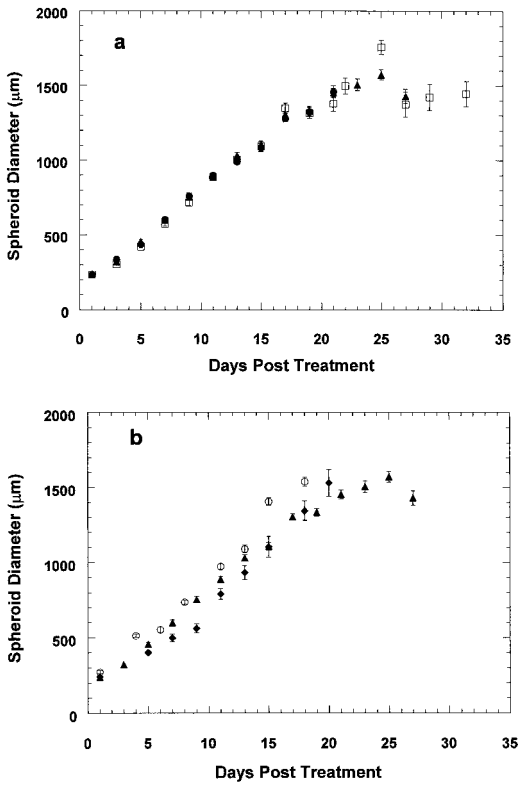

Figure 3. Growth kinetics of various control spheroids: (a) true control (no light, no drug; ●), dark control (□), light only (200 J cm^{-2}, 200 mW cm^{-2}; ▲); (b) light only (200 J cm^{-2}, 200 mW cm^{-2}; ▲), light only (100 J cm^{-2}, 25 mW cm^{-2}; ♦) and light only (25 J cm^{-2}, 25 mW cm^{-2}; ○). Each data point represents the mean of approximately 40 spheroids. Standard errors are denoted by error bars.

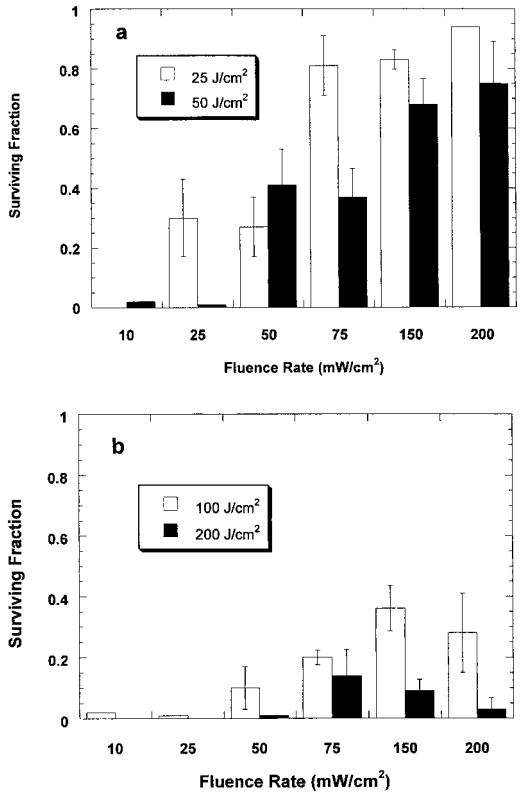

Figure 4. Spheroid survival as a function of fluence rate at representative fluences: (a) 25 and 50 J cm^{-2}; and (b) 100 and 200 J cm^{-2}. Each data point represents the mean of approximately 40 spheroids. Standard errors are denoted by error bars.

lowest fluence rate investigated here (10 mW cm^{-2}), significant spheroid kill was observed. The results presented in Fig. 4a indicate that, even at optimal fluence rates (25 mW cm^{-2}), a minimum fluence of 50 J cm^{-2} is required in order to achieve 100% spheroid kill. To achieve a comparable effect at a fluence rate of 50 mW cm^{-2} would require a total fluence of between 150 and 200 J cm^{-2} (Fig. 4b). At fluence rates of 75 mW cm^{-2} and higher, total spheroid kill could not be accomplished, even at the highest fluence (200 J cm^{-2}). To avoid hyperthermic effects, fluences in excess of 200 J cm^{-2} were not attempted.

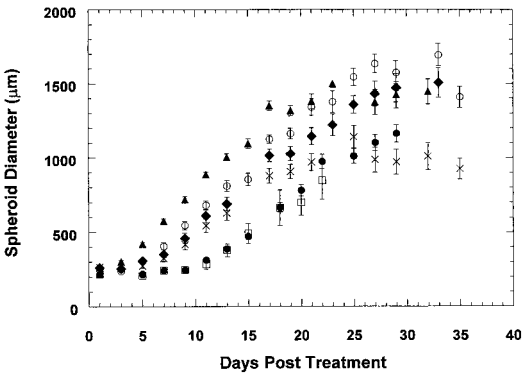

Figure 5. Growth kinetics of spheroids exposed to 25 J cm^{-2} delivered at fluence rates of: 0 mW cm^{-2} (dark control; ▲) 25 mW cm^{-2} (●), 50 mW cm^{-2} (□), 75 mW cm^{-2} (♦), 150 mW cm^{-2} (×), 200 mW cm^{-2} (○). Each data point represents the mean of approximately 40 spheroids. Standard errors are denoted by error bars.

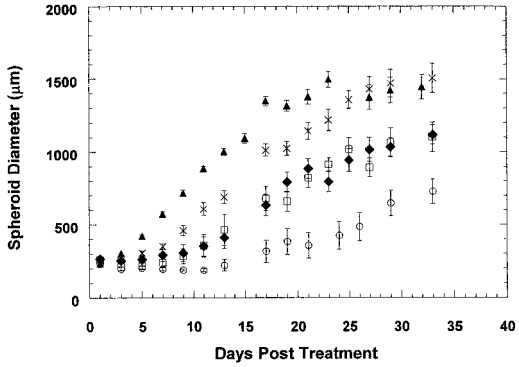

Figure 6. Growth kinetics of spheroids exposed to fluences of: 200 J cm^{-2} (○), 100 J cm^{-2} (□), 50 J cm^{-2} (♦), 25 J cm^{-2} (×) and 0 J cm^{-2} (dark control; ▲). A fluence rate of 75 mW cm^{-2} was used in all cases. Each data point represents the mean of approximately 40 spheroids. Standard errors are denoted by error bars.

The effect of fluence rate on growth delay at a fluence of 25 J cm^{-2} is illustrated in Fig. 5. Each data point represents the mean diameter of spheroids surviving a particular PDT treatment. The figure shows that there is a dose rate–dependent growth delay: longer growth delays are observed at the lower fluence rates. For example, at fluence rates of 25 and 50 mW cm^{-2} it takes approximately 15 days to reach a diameter of 500 μm, while at the higher fluence rates (>50 mW cm^{-2}), this size is attained after only 9 days.

Figure 6 shows that, for a particular fluence rate, there is a fluence-dependent growth delay; higher fluences result in significantly longer delays than lower ones. Interestingly, terminal spheroid size appears to depend on fluence as well. Spheroids exposed to 200 and 25 J cm^{-2} reach terminal sizes of approximately 700 and 1500 μm, respectively.

Although relatively small spheroids (*ca* 250 μm dia.) were used almost exclusively in these experiments, similar responses were noted following PDT of larger (*ca* 500 μm) spheroids, *i.e.* lower fluence rates are more effective (Fig. 7).

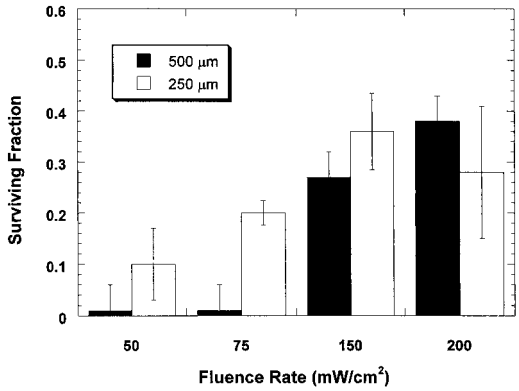

Figure 7. Survival as a function of fluence rate for spheroid diameters of: 250 and 500 μm. In both cases, spheroids were exposed to fluences of 100 J cm^{-2}. Each data point represents the mean of approximately 24 spheroids. Standard errors are denoted by error bars.

DISCUSSION

The primary finding of this study is that the response of human glioma spheroids to ALA-mediated PDT at a given fluence, is strongly dependent on the rate at which the fluence is given. The results, which are summarized in Fig. 4, are in qualitative agreement with the findings of Foster *et al.* (31) who observed significant fluence rate effects in a murine mammary carcinoma spheroid model using Photofrin®. The results of the study presented here can be interpreted by invoking the self-sensitized singlet oxygen–mediated bleaching model of Georgakoudi *et al.* (34). In this model, the details of the spatial distribution of singlet oxygen and, therefore of bleaching, depend on the fluence rate. The central prediction of this model is that, at a particular depth, singlet oxygen concentration increases as fluence rates decrease. As a result, photodynamic damage will extend further into the spheroid as the fluence rate is lowered. Thus, PDT administered at lower fluence rates will yield improved therapeutic responses since singlet oxygen is delivered to a larger volume of tumor cells.

Examination of fluence rate effects in Photofrin®-mediated PDT has been performed *in vitro* and *in vivo* by numerous investigators; however, to our knowledge, the present study is the first to attempt a systematic investigation of fluence rate effects in a human glioma spheroid model using ALA. The results presented here show that both spheroid survival and growth depend strongly on the rate at which the fluence is administered during ALA-mediated PDT. As illustrated in Fig. 4, the fluence rate effect is fluence-dependent and is more pronounced at low fluences ($\leq$50 J cm^{-2}). At higher fluences, the concentration of singlet oxygen throughout the entire spheroid volume may be sufficient to exceed the threshold for damage, regardless of the fluence rate. This is especially true if the spheroids are sufficiently small with respect to the oxygen diffusion distance. It is generally recognized that cells located within 100 μm from an oxygen source will be sufficiently oxygenated and will likely remain viable (35). Since the spheroids used in this experiment were of comparable dimension (radius $\approx$ 125 μm) to that corresponding to the maximum oxygen diffusion distance, the majority of cells in the spheroid were assumed to be viable. Thus, a lessened fluence rate effect with decreasing spheroid size would be expected due to improved oxygenation status throughout the spheroid volume. A series of experiments were performed to determine the effects of fluence rate on larger (500 μm dia.) spheroids. The results, presented in Fig. 7, are in qualitative agreement with those obtained for the smaller spheroids, *i.e.* significant fluence rate effects are observed for the large spheroids as well. In fact, the large spheroids demonstrate enhanced sensitivity to treatments at the lower fluence rates (50 and 75 mW cm^{-2}). The reason for this enhanced response is not known: it may be due to subtle differences in cell density between the large and small spheroids. At any rate, there do not appear to be significant differences in response to treatment for the two spheroid volumes considered here.

The results presented in Figs. 5 and 6 are of potential clinical relevance as they show significant fluence- and fluence rate–dependent growth delay among spheroids surviving a particular treatment. As expected, lower fluence rates induce greater growth delays than higher fluence rates (Fig. 5), while higher fluences result in greater growth delays than lower fluences (Fig. 6). Thus, even though a spheroid may survive a given treatment, its ability to grow will be adversely affected.

The two-photon fluorescence results presented in Figs. 1 and 2 show that human glioma cells synthesize Pp IX *in vitro,* thus providing a justification for ALA-mediated PDT. This observation has also been made *in vivo* by Stummer *et al.* (36) who used ALA for intraoperative fluorescence detection. Although ALA has not been used in the treatment of glioma patients, its high tumor selectivity and short cutanenous photosensitization provide compelling reasons for clinical investigations of this sensitizer.

The poor tumor selectivity observed with Photofrin® is likely the result of its inability to cross the intact blood-brain barrier (BBB) (17). Significant accumulations of Photofrin® in tumor tissues occur *via* extravasation following disruption of the BBB (15). Although Photofrin® does not cross the normal BBB, significant damage to normal brain tissue has nevertheless been observed following treatment (13,37). This is probably due to (1) microvascular damage as a result of accumulation of photosensitizer in the intact BBB (17); and/or (2) dissipation of photosensitizer with bulk flow into adjacent normal tissue traversed by edema (15). Due to the high sensitivity of normal brain tissue, there is a risk of complications during Photofrin®-mediated PDT. For example, Muller and Wilson (38) observed elevated intracranial pressures, suggestive of cerebral edema, in glioma patients treated with Photofrin®.

The results of several animal studies (17,39) show improved tumor selectivity of ALA over Photofrin®. In one study, tumor-to-white matter Pp IX concentration ratios of approximately 100 were observed in a rabbit model. This is an interesting observation since most adult tumors arise in white matter, thus providing a basis for the use of ALA in the treatment of resection margins following surgery. Although the basis for the high tumor selectivity of ALA is uncertain, there are numerous studies suggesting that ALA has the ability to traverse the intact BBB in rats (17,40–42). Conversion of ALA to Pp IX occurs in the mitrochondria. It has been suggested that porphyrin PDT is mediated by the mitochondrial benzodiazepine receptor (MBR) (43). It is likely that the converted Pp IX is confined to the outer mitochondrial membrane since it is one of the most potent binding agents to the MBR. The observation of minimal white matter damage in ALA-mediated PDT may be due to the fact that MBR is sparse in normal neuronal tissue (44). Interestingly, a 20-fold increase in the number of MBR in human gliomas compared with normal brain has been observed (44). The lack of gross propagation of Pp IX with edema into brain adjacent to tumor supports a predominantly cellular mode of localization with a negligible vascular component (36). The two-photon fluorescence images acquired in this study show localized regions of intense fluorescence surrounding the nucleus of the cell (*e.g.* Fig. 1a). Although somewhat speculative, it is entirely possible that these regions correspond to mitochondria. Studies are currently underway to identify these regions.

Several studies have demonstrated the effectiveness of Photofrin®-mediated PDT in prolonging survival in patients

with advanced brain disease. Although Photofrin® is ideally suited to one-shot intraoperative procedures, the prolonged skin photosensitivity (lasting for several weeks) may limit its usefulness in protracted treatment regimens. During this period, which represents a significant fraction of the patient's remaining survival time, the patient must be careful to avoid direct exposure to sunlight. In contradistinction, cutaneous photosensitivity following administration of ALA typically lasts approximately 24 h. Aside from the obvious improvements in quality-of-life, there is the intriguing possibility of using ALA in fractionated treatments over relatively short times without the danger of cutaneous photosensitizer build-up. The feasibility of such treatments, using indwelling balloon applicators, is currently under investigation (45).

In a previous study, measurements of light distributions from a balloon applicator immersed in a tissue-equivalent brain phantom show that it may be used to deliver sufficiently uniform light doses during PDT (45). Assuming realistic input powers of a few Watts, calculations show that it is possible to deliver adequate light doses (*ca* 50 J cm^{-2}) to depths of 1 cm in approximately 40 min (45). Of clinical relevance is that, under these treatment conditions, the dose rate at a depth of 1 cm is approximately 25 mW cm^{-2}—a dose rate that is shown by the present study to be very effective in damaging ALA-incubated human glioma spheroids. At a depth of 2 cm, however, the dose rate drops below 1.0 mW cm^{-2}, requiring approximately 22 h for adequate dose delivery. It is not known whether such low dose rates will result in sufficient PDT damage; however, it is clear that such extended treatment periods are impractical using current ''one-shot'' intraoperative PDT. Improved response to PDT may be possible through the development of new protocols involving fractionated treatments over extended time periods, perhaps even months. ALA is ideally suited to such treatments since it has a relatively short period of cutaneous photosensitivity and can be administered orally.

In conclusion, the results presented here were obtained using an *in vitro* spheroid model. Limitations of this simple model include the lack of intrinsic cell heterogeneity and the inability to account for vascular effects. The latter is especially important since a significant component of PDT damage may be mediated through the vasculature. The applicability of these results to the *in vivo* situation is not known; however, it should be noted that localized Pp IX fluorescence has been observed in glioma patients following oral administration of ALA (36). Furthermore, animal studies have shown ALA to be effective in the treatment of brain lesions (17,39). More favorable responses to lower fluence rates have also been observed in animals, albeit with Photofrin® (28). A number of issues must be addressed before ALA can be used in humans. Perhaps most importantly, it is unknown whether ALA levels in the resected tumor margin following oral administration are sufficient for the purposes of therapy. From a previous study (46) it is known that the response of human glioma spheroids to PDT is somewhat dependent on the drug concentration used. Assuming that sufficient amounts of ALA can be delivered to the cells in the resection cavity, the results of this study suggest that it may be possible to deliver light doses at suitable fluence rates to destroy glioma cells at depths of up to 1 cm in the resection cavity. There is thus the real possibility of improving local control of this aggressive and fatal disease.

Acknowledgements—The authors wish to express their gratitude to Rogelio Sanchez, Linda Lee and Eugene Chu for their experimental help. S.M. is grateful for the support of the UNLV Office of Research and the UNLV Cancer Institute. H.H. is grateful for the support of the Norwegian Cancer Society. This work was made possible, in part, through access to the Laser Microbeam and Medical Program (LAMMP) and the Chao Cancer Center Optical Biology Shared Resource at the University of California, Irvine. These facilities are supported by the National Institutes of Health under grants RR-01192 and CA-62203, respectively. In addition, Beckman Laser Institute programmatic support was provided by the Department of Energy (DOE DE-FG03-91ER61227), and the Office of Naval Research (ONR N00014-91-C-0134).

REFERENCES

1. Terzis, A.-J. A., A. Dietze, R. Bjerkvig and H. Arnold (1997) Effects of photodynamic therapy on glioma spheroids. *Br. J. Neurosurg.* **11**, 196–205.
2. Origitano, T. C., M. J. Caron and O. H. Reichman (1994) Photodynamic therapy for intracranial neoplasms: literature review and institutional experience *Mol. Chem. Neuropath.* **21**, 337–353.
3. Salcman, M. (1990) Epidemiology and factors affecting survival. In *Malignant Cerebral Glioma* (Edited by M. L. J. Apuzzo) pp. 95–109. American Association of Neurological Surgeons, Park Ridge.
4. Wallner, K. E., J. H. Galicich, G. Krol, E. Arbit and M. G. Malkin (1989) Patterns of failure following treatment for glioblastoma multiforme and anaplastic astrocytoma. *Int. J. Radiat. Oncol. Biol. Phys.* **16**, 1405–1409.
5. Cheng, M. S., J. McKean and D. Boisvert (1986) Photoradiation thereapy: current status and applications in the treatment of brain tumours. *Surg. Neurol.* **25**, 423–435.
6. Kaye, A. H., G. Morstyn and M. L. J. Apuzzo (1988) Photoradiation therapy and its potential in the management of neurological tumours. *J. Neurosurg.* **69**, 1–14.
7. Kostron, H., E. Fritsch and V. Grunert (1988) Photodynamic therapy of malignant brain tumours: a phase I/II trial. *Br. J. Neurosurg.* **2**, 241–248.
8. Muller, P. J. and B. C. Wilson (1987) Photodynamic therapy of malignant primary brain tumours: clinical effects, postoperative ICP and light penetration in the brain. *Photochem. Photobiol.* **46**, 929–936.
9. Muller, P. J. and B. C. Wilson (1990) Photodynamic therapy of malignant brain tumours. *Can. J. Neurol. Sci.* **17**, 193–198.
10. Kostron, H., A. Obwegesser and R. Jacober (1996) Photodynamic therapy in neurosurgery: a review. *J. Photochem. Photobiol. B: Biol.* **36**, 157–168.
11. Muller, P. J. and B. C. Wilson (1997) Photodynamic therapy of supratentorial gliomas. *Proc. SPIE* **2972**, 14–26.
12. Tsai, J.-C., Y.-Y. Hsiao, L.-J. Teng, C.-T. Chen and M.-C. Kao (1999) Comparative study on the ALA photodynamic effects of human glioma and meningioma cells. *Lasers Surg. Med.* **24**, 296–305.
13. Muller, P. J. and B. C. Wilson (1995) Photodynamic therapy for recurrent supratentorial gliomas. *Semin. Surg. Oncol.* **11**, 346–354.
14. Papovic, E., A. Kaye and J. Hill (1996) Photodynamic therapy of brain tumors. *J. Clin. Laser Radiat. Surg.* **14**, 251–262.
15. Stummer, W., S. Stocker, A. Novotny, A. Heimann, O. Sauer, O. Kempski, N. Plesnila, J. Wietzorrek and H. J. Reulen (1998) In vitro and in vivo porphyrin accumulation by C6 glioma cells after exposure to 5-aminolevulinic acid. *J. Photochem. Photobiol. B: Biol.* **45**, 160–169.
16. Lilge, L. and B. C. Wilson (1998) Photodynamic therapy of intracranial tissues: a preclinical comparative study of four different photosensitizers. *J. Clin. Laser Med. Surg.* **16**, 81–92.
17. Lilge, L., M. C. Olivo, S. W. Schatz, J. A. MaGuire, M. S. Patterson and B. C. Wilson (1996) The senstitivity of normal

brain and intracranially implanted VX2 tumour to interstitial photodynamic therapy. *Br. J. Cancer* **73**, 332–343.
18. Malik, Z. and H. Lugaci (1987) Destruction of erythroleukaemic cells by photoactivation endogenous porphyrins. *Br. J. Cancer* **56**, 589–595.
19. Kennedy, J. C., R. H. Pottier and D. C. Pross (1990) Photodynamic therapy with endogenous protoporphyrin IX: basic principles and present clinical experience. *J. Photochem. Photobiol. B: Biol.* **6**, 143–148.
20. Kennedy, J. C. and R. H. Pottier (1992) Endogenous protoporphyrin IX: a clinical useful photosensitizer for photodynamic therapy. *J. Photochem. Photobiol. B: Biol.* **14**, 275–292.
21. Peng, Q., K. Berg, J. Moan, M. Kongshaug and J. M. Nesland (1997) 5-Aminolevulinic acid-based photodynamic therapy: principles and experimental research. *Photochem. Photobiol.* **65**, 235–251.
22. Peng, Q., T. Warloe, K. Berg, J. Moan, M. Kongshaug, K.-E. Giercksky and J. M. Nesland (1997) 5-aminolevulinic acid-based photodynamic therapy: clinical research and future challenges. *Cancer* **79**, 2282–2308.
23. Svaasand, L. O. and R. Ellingson (1983) Optical properties of human brain. *Photochem. Photobiol.* **38**, 293–299.
24. Ben-Hur, E., R. Kol, E. Riklis, R. Marko and I. Rosenthal (1987) Effect of light fluence rate on mammalian cell photosensitization by chloroaluminum phthalocyanine tetrasulphonate. *Int. J. Radiat. Biol.* **51**, 467–476.
25. Matthews, W., J. Cook, J. B. Mitchell, R. R. Perry, S. Evans and H. I. Pass (1989) *In vitro* photodynamic therapy of human lung cancer: investigation of dose-rate effects. *Cancer Res.* **49**, 1718–1721.
26. Gibson, S. L., K. R. VanDerMeid, R. S. Murant, R. F. Raubertas and R. Hilf (1990) Effects of various photoradiation regimens on the antitumor efficacy of photodynamic therapy for R3230AC mammary carcinomas. *Cancer Res.* **50**, 7236–7241.
27. van Geel, I. P. J., H. Oppelaar, J. P. A. Marijnissen and F. A. Stewart (1996) Influence of fractionation and fluence rate in photodynamic therapy with Photofrin or mTHPC. *Radiat. Res.* **145**, 602–609.
28. Sitnik, T. M. and B. W. Henderson (1998) The effect of fluence rate on tumor and normal tissue responses to photodynamic therapy. *Photochem. Photobiol.* **67**, 462–466.
29. Sitnik, T. M., J. A. Hampton and B. W. Henderson (1998) Reduction of tumor oxygenation during and after photodynamic therapy *in vivo*: effects of fluence rate. *Br. J. Cancer* **77**, 1386–1394.
30. Sutherland, R. M., J. A. McCredie and W. R. Inch (1971) Growth of multicell spheroids in tissue culture as a model of nodular carcinomas. *J. Natl. Cancer Inst.* **46**, 113–120.
31. Foster, T. H., D. F. Hartley, M. G. Nichols and R. Hilf (1993) Fluence rate effects in photodynamic therapy of mutlicell tumor spheroids. *Cancer Res.* **53**, 1249–1254.
32. Sutherland, R. M. and R. E. Durand (1976) Radiation response of multicell spheroids—an *in vitro* tumor model. *Curr. Top. Radiat. Res.* **11**, 87–139.
33. Coleno, M. L., V. P. Wallace, C.-H. Sun, A. K. Dunn, M. B. Berns and B. J. Tromberg (1999) Two-photon exited imaging and activation of photosensitizers in tissue. *Proc. SPIE* **3604**, 67–73.
34. Georgakoudi, I., M. G. Nichols and T. H. Foster (1997) The mechanism of Photofrin photobleaching and its consequences for photodynamic therapy. *Photochem. Photobiol.* **65**, 135–144.
35. Hall, E. J. (1994) *Radiobiology for the Radiologist.* Lippincott, Philadelphia.
36. Stummer, W., S. Stocker, S. Wagner, H. Stepp, C. Fritsch, C. Goetz, A. E. Goetz, R. Kiefmann and H. J. Reulen (1998) Intraoperative detection of malignant gliomas by 5-aminolevulinic acid-induced porphyrin fluorescence. *Neurosurgery* **42**, 518–526.
37. Kaye, A. H. and J. S. Hill (1993) Photodynamic therapy of brain tumours. *Ann. Acad. Med. Singapore* **22**, 470–481.
38. Muller, P. J. and B. C. Wilson (1993) Photodynamic therapy for brain tumours. In *Photodynamic Therapy of Malignancies* (Edited by J. McCaughan), pp. 201–211. Landes, Austin.
39. Lilge, L. and B. C. Wilson (1998) Photodynamic therapy of intracranial tissues: a preclinical comparative study of four different photosensitizers. *J. Clin. Laser Med. Surg.* **16**, 81–92.
40. McGillion, F. B., G. G. Thompson, M. R. Moore and A. Goldberg (1974) The passage of δ-aminolevulinic acid across the blood-brain barrier of the rat. *Biochem. Pharmacol.* **23**, 472–474.
41. Gabriel, F., A. A. Juknat, A. M. Del and C. Batlle (1994) Porphyrinogenesis in rat cerebellum: effect of high δ-aminolevulinic acid concentration. *Gen. Pharmac.* **25**, 761–766.
42. Juknat, A. A., M. L. Kotler, A. M. Del and C. Batlle (1995) High δ-aminolevulinic acid uptake in rat cerebral cortex: effect on porphyrin biosynthesis. *Comp. Biochem. Physiol. C* **111**, 143–150.
43. Verma, A., S. L. Facchina, D. J. Hirsch, S.-Y. Song, L. F. Dillahey, J. R. Williams and S. H. Snyder (1998) Photodynamic tumor therapy: mitochondrial benzodiazepine receptors as a therapeutic target. *Mol. Med.* **4**, 40–48.
44. Shirazi, T., K. L. Black, K. Ikezaki and D. P. Becker (1991) Peripheral benzodiazepine induces morphological changes and proliferation of mitochondria in glioma cells. *J. Neurosci. Res.* **30**, 463–474.
45. Hirschberg, H., S. J. Madsen, K. Lote, T. Pham and B. J. Tromberg (1999) An indwelling brachytherapy balloon catheter: potential use as an intracranial light applicator for photodynamic therapy. *J. Neurooncol.* **44**, 15–21.
46. Madsen, S. J., C.-H. Sun, E. Chu, H. Hirschberg and B. Tromberg (1999) Effects of photodynamic therapy on human glioma spheroids. *Proc. SPIE* **3592**, 52–59.